JOURNAL OF AIRCRAFT
Vol. 29, No. 5, Sept.–Oct. 1992

Evaluation of Discrete Frequency Sound in Closed-Test-Section Wind Tunnels

Marianne Mosher*
NASA Ames Research Center, Moffett Field, California 94035

The principle objective of this study is to assess the adequacy of linear acoustic theory with an impedance wall boundary condition for modeling the detailed sound field of an acoustic source in a duct. This study compares measurements and calculations of a simple acoustic source in a rectangular concrete duct lined with foam on the walls and anechoic end terminations. Measuring acoustic pressure for 12 wave numbers provides variation in frequency and absorption characteristics of the duct walls. The study concentrates on low frequencies and low wall absorptions that correspond to measurements of low-frequency helicopter noise in a lined wind tunnel. This regime is particularly difficult to measure in wind tunnels due to high levels of the reverberant field close to the source. The standard mathematical model predicted the acoustic field poorly in the duct for the lowest frequencies, well in the near field of the higher frequencies, and inconsistently in the far field of the higher frequencies.

Nomenclature

A_n = coefficient for source expansion
a = radius of source
C_α = wall absorption coefficient for normal incidence
c = speed of sound in fluid
d = distance from source axis, $\sqrt{x^2 + z^2}$
dB = $20 \log(p_{\text{rms}}/p_{\text{ref}})$
f = function defining acoustic source
$\boldsymbol{H}$ = matrix of eigenmodes for duct
h_n = Hankel function
i = $\sqrt{-1}$
k = wave number of acoustic field, ω/c
$\boldsymbol{k}$ = diagonal matrix of axial duct wave numbers
l = typical duct cross dimension, square root of duct cross-section area
n = normal to surface
P_n = Legendre polynomial
p = Fourier coefficient of acoustic pressure at one frequency
$\boldsymbol{p}$ = vector of acoustic pressure at control points on an outflow boundary
p_s = Fourier coefficient of acoustic pressure due to source at one frequency
r = distance from source
z = specific acoustic impedance of wall
θ = angle from $+y$ axis
φ = angle in horizontal plane from $-z$ axis
ω = acoustic frequency, radians/sec

Introduction

WIND-tunnel tests with acoustic measurements can provide useful information in the design and development of aircraft. Researchers use wind tunnels to study basic aeroacoustic phenomena, test prototypes and design concepts, and test flight vehicles. The standard hard-walled wind tunnel creates an adverse environment for making acoustic measurements, due to interference from wall reflections and high background noise levels. Acoustically absorbent linings, permanently or temporarily mounted, have been used to reduce the interference due to reflections in many wind tunnels including the 40- × 80-ft, 80- × 120-ft, and 7- × 10-ft wind tunnels at NASA Ames Research Center; the 8- × 6-ft transonic wind tunnel at NASA Lewis Research Center; the 20- × 20-ft low-speed wind tunnel at Boeing Helicopter Company; and the Vought 7- × 10-ft low-speed wind tunnel. Understanding the acoustic properties of these wind tunnels is important for the researcher making acoustic measurements within these facilities. Understanding also provides critical information for modifying or designing any new closed-test-section wind tunnel that will be used to make acoustic measurements.

In the early part of the 20th century, Sabine[1] recognized the problem of interference of reflected waves in an acoustic field in a closed space. He studied the problem in rooms experimentally and developed an analysis relating reverberation to a room's geometry and the absorption characteristics of surfaces. More recently, Tyler and Soffrin[2] developed an acoustic analysis to study fan noise in a hard circular duct based on modal propagation. A similar model was developed to study jet engine noise suppression with the inclusion of impedance boundary conditions.[3] This model has been tested for its prediction of axial acoustic pressure attenuation and spatial mode shapes.[4–7] Attenuation of a single mode was sometimes well predicted and sometimes not so well predicted. Mode shapes were predicted well for very low-order axial modes in circular ducts, but not for radial modes or high-order modes. Eversman and Baumeister[8] used the same physical model, the wave equation with impedance boundary condition, to study the acoustic field of a propeller in a circular wind tunnel. Their analysis (convected wave equation with impedance boundary condition on wall) is similar to the one developed by this author,[9] yet solved by a different method.

An analytical model and computer program were developed to analyze the reflection problem in wind tunnels.[9] This analysis can be used to determine where uncontaminated measurements can be made for a particular test installation in a wind tunnel or what wall treatment is needed to obtain a given acoustic performance. The purpose of the research

Presented as Paper 90-4011 at the AIAA 13th Aeroacoustic Conference, Tallahassee, FL, Oct. 22–24, 1990; received Feb. 11, 1991; revision received Sept. 13, 1991; accepted for publication Sept. 13, 1991.

*Aerospace Engineer.

reported here is to evaluate the applicability of the model to study the effect of the wind tunnel wall reflection on discrete low-frequency noise measurements typical of helicopter rotor rotational noise. Previously,[9] the ability of the computer program to solve the modeled equation and boundary condition was found accurate by comparing computed results with an analytic solution for a point monopole in a duct. Since the model of the convected wave equation and impedance boundary condition is used in Refs 3–9, the assessment reported here applies to this previous work as well as the modeling of this author.[9]

To evaluate the model requires first measuring the acoustic field of the source in the free field with no reflection and in a duct with known acoustic properties, and then comparing the measured effect of the duct on the acoustic field with predictions. Figure 1 outlines the steps used to evaluate the analytical model in this study. The radiation pattern of the single frequency acoustic source was measured in an anechoic chamber. These measurements provide both the baseline measurements of the source for determining the effect of the duct experimentally and the information necessary for an analytic description of the source of the theory. Acoustic measurements were then taken with the same source in the duct. The difference between these measured acoustic fields is the effect of the duct. Predictions were made using measured acoustic properties of the duct surface and the source. Comparing the predicted effect of the duct with the measured effect of the duct then shows how well the theory predicts discrete frequency sound propagation in the duct.

Experiment

The acoustic field surrounding a source was measured in an anechoic chamber and in a duct. The difference of the two acoustic fields shows the effect of the duct. The experiment simulates a one-tenth scale version of the NASA Ames 40- × 80-ft wind tunnel, if a rectangular test section is used. The nondimensional parameter for matching frequency and size is kl, k is the wave number, and l is a typical length. For this study, l is the square root of the cross-section area. Similar geometry with a constant kl contains the same number of wavelengths per wind tunnel size. In this study, kl ranges from 8.52 to 26.46 (see Table 1); for each value of kl, multiple modes will propagate in the duct. When scaled up to a rectangular 40- × 80-ft cross section, this range of kl corresponds to frequencies of 27–84 Hz. Absorption of sound waves perpendicular to the wall by the foam lining in the duct ranges from about 0.1 to 0.25. Predictions of absorption of the 40- × 80-ft wind tunnel for these frequencies range from 0.16 to 0.38 with the current 0.152-m (6.0-in.) liner.

Physical Setup

Anechoic Chamber

Wedges with a normal absorption coefficient greater than 0.99 above 125 Hz cover most of the chamber. No wedges cover a jet nozzle, collector, and a section of the floor containing mounting hardware. These regions were covered with foam. A steel grid floor in the chamber allows access to the chamber and reflects some sound. The walls of the chamber have an isolation of 37 dB at 125 Hz and 73 dB at 4800 Hz.[10]

Duct

Figure 2 shows the duct, a 6.096-m (20-ft)-long rectangular concrete section with interior dimensions of 1.219-m (4-ft) wide by 2.438-m (8-ft) high. The walls are 0.152-m (6-in.) thick with a reinforcing grid of steel in the middle. Epoxy paint and one inch of foam cover the interior walls. Mylar sheeting covers the exposed exterior surfaces to help keep the interior a uniform temperature by reflecting solar radiation. Both ends consist of wooden doors covered by foam wedges (same wedges as in the anechoic chamber) on the interior designed to absorb sound so the finite length duct will mimic an infinite length duct. A hole in one wall of the duct allows the acoustic source and microphone traverse to be positioned inside the duct. Two 0.305-m (12-in.)-diam fans circulated air within the duct between measurements to reduce temperature gradients.

Acoustic Source

The acoustic source has sound radiating from the open end of a 1.219-m (4-ft)-long, 5.08-cm (2-in.)-diam aluminum tube attached to a speaker. This configuration was chosen because at resonances of the tube the hard walls of the duct produced minimal effects on the acoustic output of the tube.

Instrumentation

Acoustic measurements were made with 1.27-cm (0.5-in.) condenser microphones. A reference microphone was placed at the end of the source tube parallel to the tube with the sensor 0.64-cm (0.125 in.) in front of the tube. A survey was taken with another microphone mounted on a traverse that was attached to the source. Microphone signals were monitored on an oscilloscope and root mean square voltmeter. Measurements, taken with a two-channel analyzer, consist of the transfer function from the reference microphone to the survey microphone. Results were stored on disks on a personal computer. The computer controlled the analyzer in the data acquisition and provided the electric signal to drive the speaker in the acoustic source.

Measurements

Measurements were made at six pairs of wave numbers: kl = 8.52 and 8.61; 12.5 and 12.6; 16.2 and 16.4; 19.7 and 19.9; 22.8 and 23.0; and 26.2 and 26.5. The wave numbers and frequencies in a pair differ by 1% and are spaced at resonances of the tube to provide good signal-to-noise ratio. By making measurements and calculations in pairs, the sensitivity of the system to small changes in wave number can be found. Making

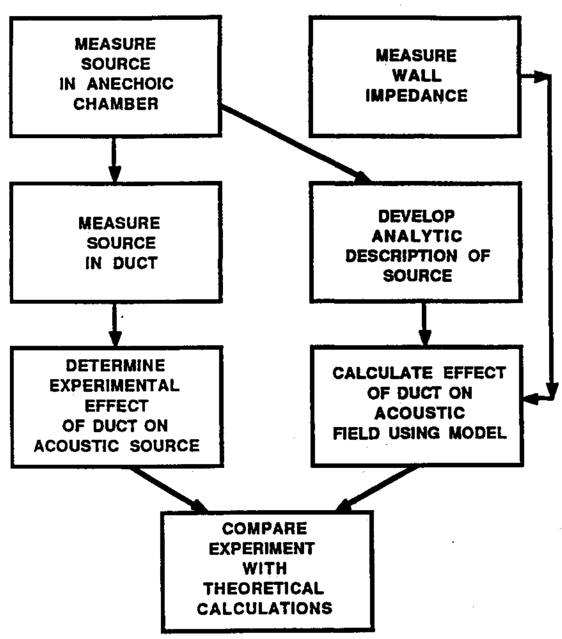

Fig. 1 Steps to evaluate analytical model in this study.

Table 1 Wave numbers and frequencies tested

ka	kl	k, 1/m (1/ft)	Frequency at 70°F Hz	No. propagating modes	No. modes modeled
0.1255	8.52	4.94 (1.51)	270.4	7	50
0.2360	16.23	9.41 (2.87)	514.8	23	162
0.3358	22.80	13.22 (4.03)	723.3	42	338

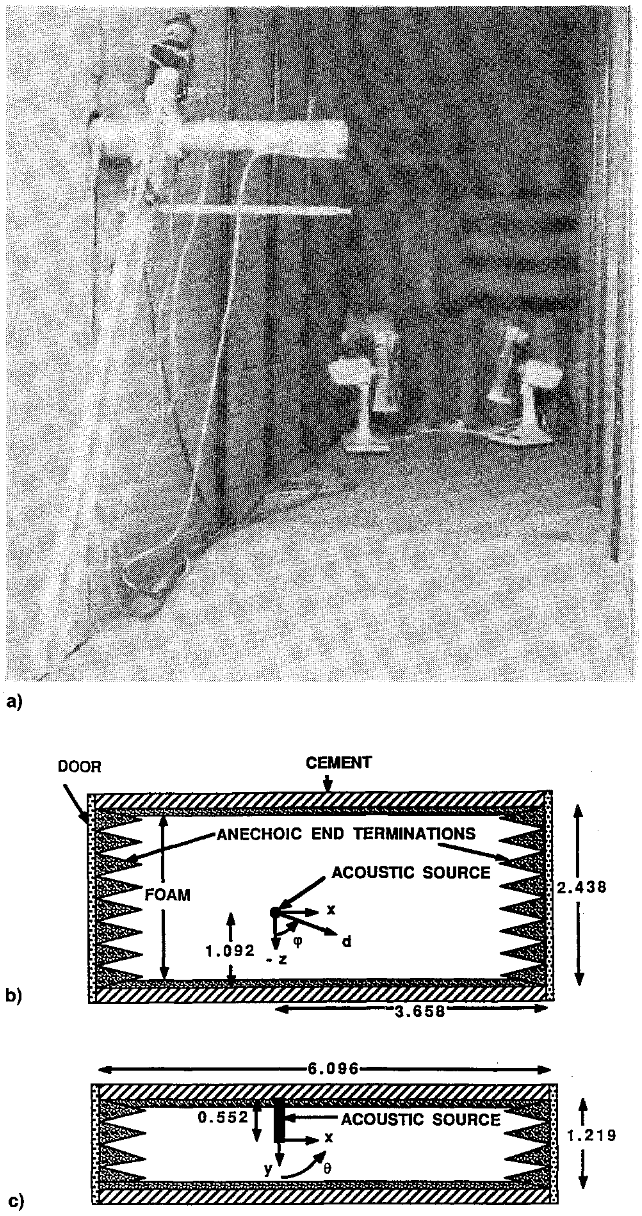

Fig. 2 Duct: a) inside; b) side view; and c) top view.

transfer function measurements corrects for any amplitude variation in the output of the source to best match the assumptions in the theory being evaluated. Microphones were calibrated with a pistonphone, and relative humidity was measured each day before testing. Temperature was monitored continuously with three thermocouples, placed at the level of the source, 0.762 m (2.5 ft) above the source, and 0.762 m (2.5 ft) below the source. The average of the three temperatures was taken to be the duct temperature. Data were acquired only when the maximum temperature difference was 0.6°C, and usually the temperature difference was less than 0.3°C. Vertical temperature differences in the anechoic chamber were much smaller than in the duct, so mixing the air was not needed.

Primary Measurements

Acoustic measurements in a plane 2.54 cm (1 in.) in front of the source provide a definition of the acoustic field radiating from the source in the anechoic chamber. Measurements were also taken in the duct in a plane 2.54 cm (1.0 in.) in front of the source, along radial lines from 0 to 0.914 m (36 in.). The radial sweeps were repeated at 30-deg increments. Actual microphone locations were measured and used in the calculations. Subtracting measurements made in the anechoic chamber from measurements made in the duct gives the effect of the duct.

Table 2 Specific acoustic impedance boundary conditions and resulting absorption coefficients

kl	z	C_α
8.52	(1.241, −7.270)	0.086
8.52	(1.427, −7.663)	0.088
8.52	(1.465, −7.649)	0.091
16.23	(0.551, −3.998)	0.120
16.23	(0.590, −4.091)	0.122
16.23	(0.550, −3.852)	0.128
22.80	(0.414, −2.875)	0.161
22.80	(0.559, −2.936)	0.202
22.80	(0.579, −2.785)	0.229

Other Measurements

Measurements very close to the source in the anechoic chamber provide a reference to compare with similar measurements in the duct to check for influence of the duct on the output of the source. In the anechoic chamber, measurements made near and far from the source in many directions provide input for an empirically derived analytic expression for the radiated acoustic field used in the computations.

To obtain the impedance boundary condition, the impedance at normal incidence of the foam lining was measured with an impedance tube (see Ref. 11 for details). At least two (usually three or more) measurements were made of each wave number for the foam sample. For each of the 12 wave numbers used with the 2.54-cm (1-in.) foam, impedance measurements were made on at least two different days. Data scatter is larger for the higher wave numbers, so more data were collected for the higher wave numbers. Boundary conditions from measured impedances for the samples with minimum, maximum, and median absorptions were used in the calculations (see Table 2).

Analysis

Source Model

The acoustic source is modeled as an arbitrary point source producing outgoing waves of one frequency; a series expansion in spherical coordinates represents this model mathematically. Measurements in the anechoic chamber indicate the acoustic field is independent of the angle φ. Truncating the series expansion for this arbitrary point source produces an excellent approximation for real sources since all significant terms are kept:

$$p_s(r, \theta, \varphi, k) = \sum_{n=1}^{N} A_n h_n(kr) P_n(\cos\theta) \qquad (1)$$

This acoustic source, radiation from an open tube with a small radius compared to the wavelength (ka = 0.1255–0.3897), is expected to produce a simple radiation pattern that will be well represented with a few terms. Measurements made in the anechoic chamber support the symmetry assumption. The coefficients for modeling the acoustic source were determined by measuring the radiation pattern and fitting the coefficients with a least squares curve fit. Once the coefficients are known, the harmonic amplitude of the acoustic pressure can be estimated everywhere in free space with Eq. (1). Reference 11 gives more details of the source model.

Duct Model

To study how a closed-test-section wind tunnel alters the sound field from an acoustic source, a simplified model containing the relevant physics and amenable to solution using a computer was developed. References 9 and 12 detail the model's development and solution. This section briefly describes the model.

The model in this study uses the standard description of sound propagation in air of the convected wave equation, or the Helmholtz equation[13] in the frequency domain. The convected wave equation and the Helmholtz equation have been used successfully for many years to describe low-amplitude sound propagation in uniform air. Examples in this study contain no flow, so they can be described by the Helmholtz equation:

$$\nabla^2 p + k^2 p = f \tag{2}$$

Walls are modeled with the standard impedance boundary condition[13] that relates the acoustic pressure to the acoustic velocity normal to the boundary at a point:

$$p = \left(\frac{-i}{k}\right) z \frac{\partial p}{\partial n} \tag{3}$$

This allows the boundary to absorb some acoustic energy. Since this boundary condition is a local condition that specifies properties at an individual point, it does not allow for the interaction of the acoustic waves in the air with any propagating waves that could be induced in the boundary medium. Neither elastic waves propagating in the structure nor acoustic waves propagating in the lining or the boundary layer are accounted for in this model. The duct modeled is infinitely long. Outflow boundary conditions were determined from modal propagation away from the source:

$$\frac{\partial p}{\partial n} = Hikp \tag{4}$$

This outflow boundary condition ensures wave propagate away from the source in the duct with a constraint on the acoustic pressure and its spatial derivative.

Adequacy of Model Assumptions

Although the experiment was specifically designed to match the analytical model, some idealized aspects of the source and duct models cannot be created in the real world.

The analytic source model consists of a point source radiating outward with cylindrical symmetry (a radiation pattern from low-order poles) that is unaffected by the duct. The real source extends over a finite region. Measurements close to the actual distributed source do not match a simple point source model. Measurement locations closer than 0.1016 m (4 in. or two source diameters) from the center of the source were not used in the analytic source model, thus allowing a much better fit to the source model with all other measurements. These differences should not be important to this test because they only affect the sound filed due to the source in the region closest to the source and thus do not affect the reflections. Measurements near the source reveal the symmetry assumption to be good. The second-order curve fit, monopole plus dipole, fits the measurements about as well as the eighth-order curve fit. The difference between the measurement and the curve fit of the analytical model subsequently used in the predictions is usually less than 0.5 dB, but reaches 2.5 dB for a few (<2%) locations and wave numbers. The form of the model is good for describing the radiated acoustic field. Measurements very close to the source in and out of the duct show the duct has little effect on the radiation from the source.[11] In summary, the analytical source model simulates the source very well for this study.

The duct model assumes linear acoustic waves propagate in a uniform ideal gas in an infinitely long rectangular duct with side walls that reflect the sound like a point impedance. The acoustic waves are linear since their maximum amplitude is 80–90 dB. The air was uniform except for a small vertical temperature gradient. Data collection was restricted to a temperature difference of 0.6°C over the 1.524-m (5-ft) distance between the upper and lower thermocouple in the duct. This maximum temperature difference corresponds to less than a 0.2% change in speed of sound and wave number. The duct is a finite length designed with nonreflecting ends. The source was placed asymmetrically in the duct so reflections from the ends would produce asymmetry in the measured data. Thus symmetry in the measured data indicates the ends of the duct effectively mimicked an infinitely long duct. The duct model does not include reflections off the source tube. In this study, the wavelength is large compared to the source tube, so the tube is an inefficient scatterer of sound and thus is expected to have little effect on the sound field in the duct. The impedance boundary condition models the effect of the lined duct walls on the acoustic field. It describes the sound wave at the surface as moving with a velocity proportional to the acoustic pressure, but does not account for any wave propagation in the surface. This boundary condition has been widely used by other researchers (Refs. 3, 6, 8, and 13). The value of the wall impedance was determined by measuring the impedance of the lining in an impedance tube. Differences in the acoustic impedance of the back of the impedance tube (steel plate) and the duct (painted concrete) would affect the accuracy of the measurement. Scatter in the measured absorption exceeds the difference between steel and concrete. Scatter in the measured impedance produced only a very small difference in predictions.

Results

The test included 12 wave numbers grouped as 6 wave number pairs. This paper contains results for 3 wave numbers; Ref. 11 contains results for all 12 wave numbers tested. Table 1 lists the basic characteristics of these 3 wave numbers, including the number of modes used in the analytical model to represent the outflow boundary conditions and the number of modes that propagate in the duct as modeled. Table 2 lists the specific acoustic impedance and absorption coefficients used in the calculations.

The acoustic field in the duct can be divided into three regions. First, a localized region exists very near the source where the direct acoustic field of the source strongly dominates. In this test only the central point at 0 m distance from the source axis and 2.54 cm (1 in.) in front of the source lies in the localized region. Second, a duct near field region extends farther from the source where the reverberant field combines with the direct acoustic field, thereby modifying the acoustic field smoothly up to a few dB. In the duct near field, the acoustic pressure in the duct is above or below the acoustic pressure without the duct around the source depending on whether the reflected acoustic field combines coherently or incoherently with the direct acoustic field from the source. For the lowest wave number, locations out to about 0.152 m (6 in.) from the source lie in the duct near field and for the highest wave number, locations out to about 0.381 m (15 in.) from the source lie in the duct near field. Third is a duct field where the reverberant field dominates with a complicated acoustic field containing modal propagation in the duct.

Figures 3, 4, and 5 illustrate a detailed comparison between the measurements and calculations for the first, fifth, and ninth wave numbers (kl = 8.52, 16.23, and 22.80). All data, measurements and three calculations, are plotted along radial lines. Curves show the difference in sound pressure level (SPL) with and without the duct around the source. This parameter establishes the effect of the reverberant field on the acoustic field in the duct; it is zero where the reflected field is not interfering, positive where the reflected field combines coherently, and negative where the reflected field combines destructively with the acoustic field radiating from the source.

Data for the first wave number (Figs. 3a and 3b) represent data for the first four wave numbers (kl = 8.52–12.58). The

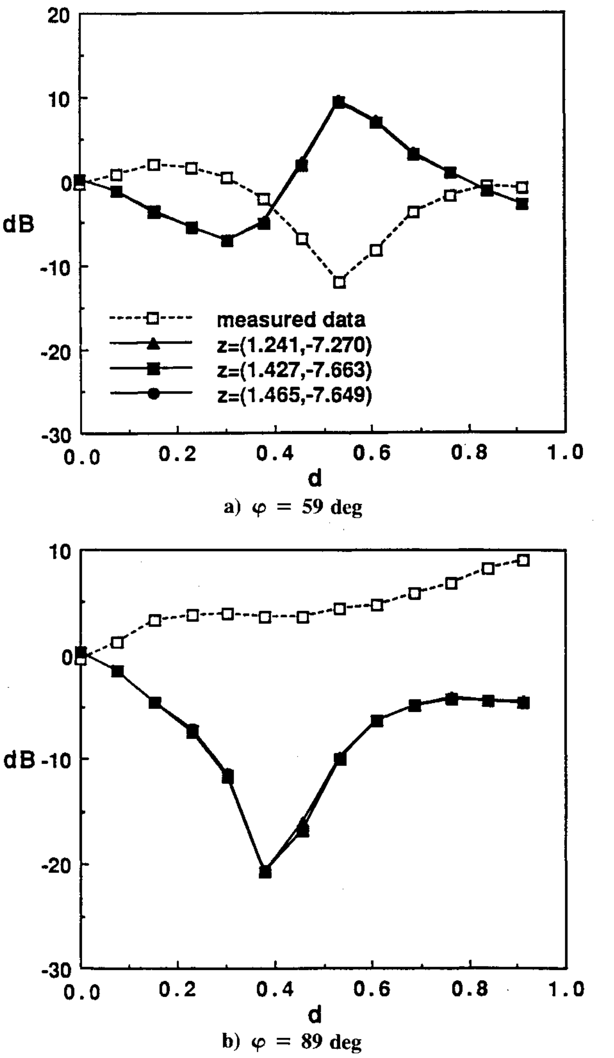

Fig. 3 Measurement and predictions of the difference between SPL in duct and anechoic chamber kl = 8.52.

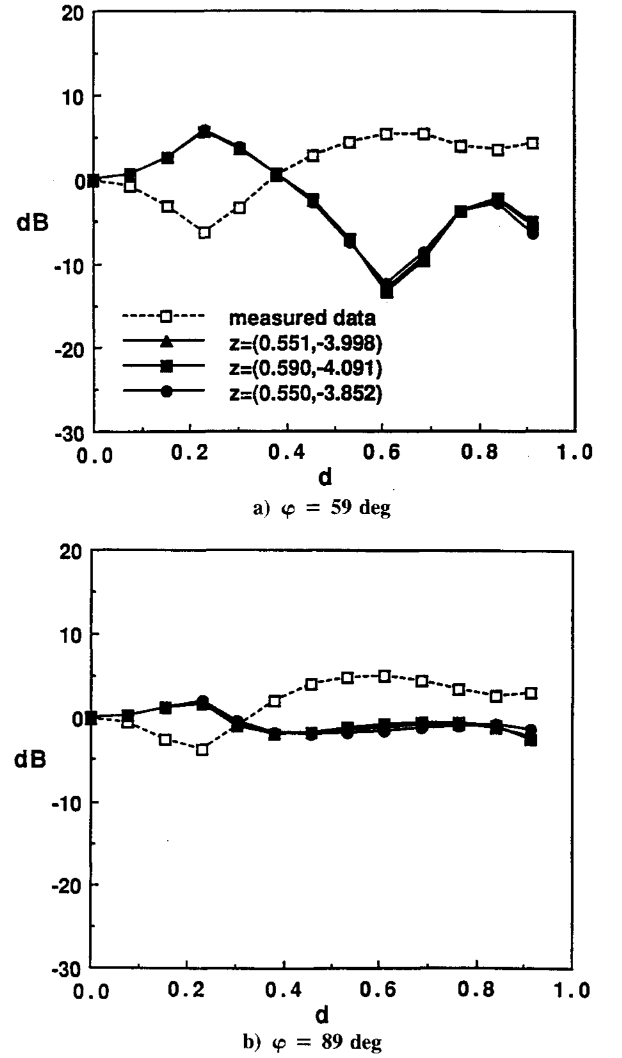

Fig. 4 Measurement and predictions of the difference between SPL in duct and anechoic chamber kl = 16.22.

data exhibit very poor correlation between calculation and measurement except at the center point where the computations are nearly identical with the measurements. Measured trends differ from calculated trends in both the duct near and far fields. The three computations (C_α = 0.086, 0.088, and 0.091) are nearly identical.

Data for the fifth wave number (Figs. 4a and 4b) represent data for the fifth and sixth wave numbers (kl = 16.23 and 16.90). At some angles, the data exhibit poor correlation between calculation and measurement except near the center point where the computations are nearly identical with the measurements. At some angles the measurements correlate well with the computations. Measurements match calculations well in some duct near-field locations and show similar trends at other duct near-field locations. Measurements sometimes match calculations well and sometimes exhibit different trends in the duct far field. The three computations (C_α = 0.120, 122, and 0.128) are nearly identical.

Data for the ninth wave number (Figs. 5a and 5b) represent data for the seventh through tenth wave number (kl = 19.68–23.03). Measurements match calculations well in the localized and duct near fields. Measurements sometimes match calculations well and sometimes exhibit different trends in the duct far field. The three computations (C_α = 0.161, 0.202, and 0.229) exhibit some differences. These differences remain small except at extremes of pressure with steep gradients.

Calculations predicted the localized very near-field well in all cases studied. Calculations predicted the duct near field poorly for the lowest wave numbers, increasingly better as the wave number increased from kl = 8.52 to 23.02, then not as well for the two largest wave numbers, kl = 26.20 and 26.46 (data in Ref. 11). At the lower wave numbers (kl = 8.52–16.23), the reverberant field was not always well predicted; whereas, at the higher wave numbers (kl = 16.90–23.03), the reverberant field was well predicted in the near field. Calculations predicted the duct far field poorly for the lower wave numbers and moderately well for the higher wave numbers. At the lower wave numbers calculated acoustic fields have little resemblance to measured far fields. At larger wave numbers the calculations show more resemblance to the measurements.

Sensitivity Study for Test Parameters

Results of the correlation depend on the accuracy to which the parameters are known. This study checked for the influence on the results of small changes to the speed of sound, wall boundary conditions, source model, and locations of the microphones and the acoustic source. Small errors in measurement do not account for the discrepancy between measurements and calculations in this study. Details are in Ref. 11.

Discussion

Comparison of Calculations with Measurements

This validation effort demonstrated that the analysis (linear wave equation with impedance boundary condition on walls) used in the calculations can predict the effect of an enclosure

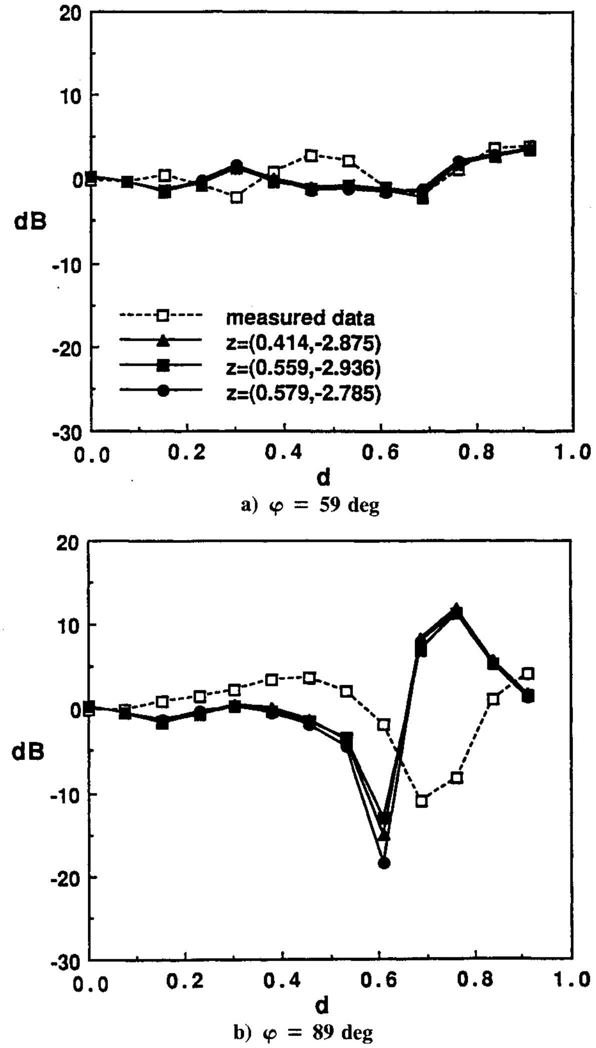

Fig. 5 Measurement and predictions of the difference between SPL in duct and anechoic chamber kl = 22.80.

on the acoustic field of a known source for some cases. The analysis worked better for the higher wave numbers that exhibit a higher lining absorption for a given depth of foam. The model does not work well for very low frequencies with low absorption. The model itself requires more computer time and memory to calculate as the nondimensional product kl of the wave number and duct cross dimension increases. Thus, this computation becomes less useful for higher frequencies.

Poor Correlation for Low Wave Numbers

In acoustically absorbent linings, viscous fluid damping converts acoustic energy into heat as the acoustic waves interact with the fine structure of the lining. In this study, predictions of acoustic interactions with the foam lining are based on an impedance model that assumes the pressure and velocity perturbations are in phase with a ratio of $\rho_0 c$ for the incident acoustic wave. In the acoustic near field of a source the relationship between pressure and velocity perturbations is more complicated. For the simplest source, an acoustic monopole, the pressure and radial velocity perturbations behave as

$$p \propto \frac{p_0 c e^{ikr}}{r}, \quad v \propto \frac{e^{ikr}}{r}\left(1 + \frac{i}{kr}\right) \tag{5}$$

Measurements of the impedance were done with a plane-propagating wave and thus do not account for an extra out-of-phase acoustic near-field velocity perturbation in the incident, nearly spherical wave. Thus the boundary condition used in this analysis does not model acoustic interactions at a wall in the source near acoustic field. This may explain why correlation of predictions and measurements is so poor for the lowest wave numbers.

More detailed measurements of the acoustic field in the duct would show how the boundary was behaving. In particular, acoustic pressure and pressure gradient measurements at the walls of the duct would show if the wall impedance in place differed from the impedance measured in the standing wave tube. If the acoustic near-field velocity caused these impedances to differ from far-field measurments, the measured impedance would be different at different parts of the duct, depending on how far that wall was from the source. If the interaction of the acoustic near field with the boundary is the cause of poor correlation at small wave numbers, a different theory would need to be developed to analyze these cases.

Implications for Using Analysis

This study evaluated the validity of the analysis (linear wave equation with impedance boundary conditions on walls) to predict wall reflection effects for low-frequency simple sources and simple ducts lined with foam that have low absorption of sound waves. The analysis can predict the local region about a source where the reverberant field is minimal or causes variations of less than 1 dB. At absorption levels above 0.12 and for wave numbers with $kl > 16.90$, the analysis did well at predicting the extent of the duct near field and the effect up to about 5 dB but loses accuracy at the lower frequencies ($kl < 16.23$). This means the analysis is good for defining the volume where acoustic data can be taken with no or little interference from the wall reflections in a given wind tunnel setup and for comparing the duct near-field acoustic characteristics of different wind tunnels, except at very low frequencies. Since the analysis accurately predicts the duct near field for wave numbers with $kl > 16.90$ when the absorption level is above 0.12, it could be developed into a wind tunnel wall correction scheme for some situations. The analysis does not provide consistent accurate duct far-field predictions where wall effects dominate the acoustic field, so it is not suitable for a far-field correction scheme.

Work Needed to Further Validate Analysis

This work examined the validity of the analytical model in an idealized experiment with low to medium frequencies (kl = 8.52–26.48) and low normal absorptions (C_α = 0.088–0.264). More experimentation with moderate (up to 0.8) and high (up to 0.95) absorptions is needed to test the analysis in regions with higher absorptions. Since the predictions improved with increased wall absorption in this study, the analysis can be expected to do well at predicting the local and duct near acoustic fields for a simple source in a duct with moderate and high absorption.

Testing the model in a real wind tunnel instead of an idealized experiment is a final step required to evaluate the usefulness of the model. The expected outcome of such a test is that the correlations would remain good for the local field, degrade slightly in the duct near field, and deteriorate in the duct far field.

Conclusions and Recommendations

A study was conducted to test the adequacy of linear acoustic theory with a point impedance wall boundary condition for modeling effects of walls on the acoustic field in ducts. The model had been developed to study the effects of wall reflections on acoustic measurements in closed-test-section wind tunnels, especially low-frequency helicopter noise. This study compares measurements and calculations of a simple acoustic source in a rectangular concrete duct containing foam on the walls and anechoic end terminations. Measuring acoustic pressure for six pairs of wave numbers (12 wave numbers total) provides variation in frequency and absorption characteristics of the duct walls. The conclusions from this study are:

1) The linear acoustic theory with a point impedance wall boundary condition provided poor predictions of the duct acoustic field for low frequencies of $kl < 16.9$. The discrepancy is believed to be due to the inadequacy of the impedance model of the wall when the wall is in the acoustic near field of the source.

2) The linear acoustic theory with a point impedance wall boundary condition accurately predicts the effect of lined duct walls on a source in the duct near field for values of wave number times cross-section dimension of $kl = 16.9–26.5$ and absorptions of $C_\alpha = 0.124–0.265$. The duct near field is the volume surrounding the source where reflections alter the acoustic field less than 5 dB and in a smooth way. The analysis probably will predict well in the duct near field for higher absorptions with $kl > 16.9$.

3) The linear acoustic theory with a point impedance wall boundary condition provided general characteristics but not accurate details of the duct far field for $kl > 16.9$. No application of this theory is likely to be adequate for accurately predicting the details of the duct far field in a duct where modal propagation dominates. The duct far field is the volume away from the source where the acoustic field is dominated by the reflections so the field no longer resembles the field radiated by the source without boundaries. With many propagating modes far from the acoustic source, small changes in any mode shape or amplitude can change the details of the acoustic field significantly. This requires a very accurate computation of the duct acoustic modes that are sensitive to duct size, shape, and boundary, and a very accurate computational description of the free field of the acoustic source.

The recommendations from this study are:

1) The analytical model should be checked for its validity in predicting the duct near field with moderate and high levels of absorption.

2) To gain a better understanding of why the analysis fails at the low frequency, the acoustic field in the duct should be measured in more detail. Acoustic intensity measurements throughout the duct and especially near the walls might be very helpful.

3) If an analysis is needed to predict the near acoustic field of a low-frequency source ($kl <$ about 17) in a duct, a better model needs to be developed. In particular the point impedance boundary condition appears to be inadequate in this regime and a more accurate model needs to be developed.

4) Predictions from the analytical model should be validated with data obtained in a real wind tunnel with wind and a finite length test section.

References

[1]Sabine, W. C., *Collected Papers on Acoustics*. Dover Publications Inc., New York, 1964, reproduction from Harvard University Press, 1922.

[2]Tyler, J. M., and Sofrin, T. G., "Axial Flow Compressor Noise Studies," Preprint 345D SAE Natl. Aero. Meeting, New York, April 1961, pp. 309–322.

[3]Rice, E. J., "Attenuation of Sound in Soft Walled Circular Ducts," NASA TM X-52442, 1968.

[4]Feiler, C. E., and Rice, E. J., "Performance of Inlet Sound Suppressors," NASA SP-189, 1968, pp. 53–62.

[5]Liu, H. K., and Martenson, A. J., "Optimum Lining Configurations," NASA SP-207, 1969, pp. 425–434.

[6]Plumblee, H. E., "A Theoretical and Experimental Study of Sound Attenuation in an Annular Duct," AIAA Aeroacoustic Conf., AIAA Paper 73-1005, Seattle, WA, Oct. 1973.

[7]Plumblee, H. E., Dean, P. D., Wynne, G. A., and Burrin, R. H., "Sound Propagation in and Radiation from Acoustically Lined Flow Ducts: A Comparison of Experiment and Theory," NASA CR-2306, 1973.

[8]Eversmann, W., and Baumeister, K. J., "Modeling Wind Tunnel Effects on the Radiation Characteristics of Acoustic Sources," *Journal of Aircraft*, Vol. 23, No. 6, 1986, pp. 455–463.

[9]Mosher, M., "The Influence of Wind-Tunnel Walls on Discrete Frequency Noise," Ph.D. Thesis, Stanford Univ., Stanford, CA, June 1986.

[10]Soderman, P. T., Unpublished data on characteristics of anechoic chamber at Ames Research Center, 1975.

[11]Mosher, M., "Validation Study of an Analytical Model of Discrete Frequency Sound Propagation in Closed-Test-Section Wind Tunnels," NASA TM-102801, 1990.

[12]Mosher, M., "Effect of a Wind Tunnel on the Acoustic Field from Various Aeroacoustic Sources," AIAA 10th Aeroacoustics Conf., AIAA Paper 86-1897, Seattle, WA, July 1986.

[13]Morse, P. M., and Ingard, K. U., *Theoretical Acoustics*, McGraw-Hill, New York, 1968.